Paper AAS 98- 183

ASTEROID SELECTION AND MISSION DESIGN FOR SPACEDEVCO'S NEAR-EARTH ASTEROID PROSPECTOR

Christopher R. Cassell, Alan M. Schneider, Russell Gulman, Regis Lee, and Ethan Estey

Near-Earth Asteroid Prospector will be the first privately financed deep-space mission, the start of a series from SpaceDevCo. The requirements for an early completion of a profitable voyage dictate formidable challenges for the preliminary design team of students and their mentors at the California Space Institute of the University of California, headquarted at the San Diego campus in La Jolla. Nevertheless, a member of asteroid rendezvous opportunities exist within the constrains of cost, time, delta-v, weight, power, etc. This paper focuses on criteria and modeling tools for asteroid selection, as well as the launcher and escape trajectory planning.

AAS/AIAA Space Flight Mechanics Meeting

Monterey, California 9–11 February 1998

AAS Publications Office, P.O. Box 28130, San Diego, CA 92128

ASTEROID SELECTION AND MISSION DESIGN FOR SPACEDEV'S NEAR-EARTH ASTEROID PROSPECTOR

Christopher R. Cassell[+], Alan M. Schneider[*], Russell Gulman[++], Regis Lee[++], and Ethan Estey[++]

Near-Earth Asteroid Prospector (NEAP) will be the first privately financed deep-space mission, the start of a series from Space Development Corporation. The requirements for an early completion of a profitable voyage dictate formidable challenges for the preliminary design team of students and their mentors at the California Space Institute of the University of California, headquarted at the San Diego campus in La Jolla. Nevertheless, a number of asteroid rendezvous opportunities exist within the constraints of cost, time, delta-v, weight, power, etc. This paper focuses on criteria and modeling tools for asteroid selection, as well as the launch vehicle requirements and escape trajectory planning.

INTRODUCTION

The Space Development Corporation plans to send a spacecraft (s/c) to rendezvous with a near-earth asteroid within the next three years. The objective of the first of several such missions is to "see it, characterize it, touch it" in the words of Jim Benson, founder of SpaceDev, Inc. A guiding principle for the design is that this first privately financed mission outside the earth's neighborhood be done at low cost on an accelerated timetable. The design of the s/c and all the preceding stages must therefore be kept as simple as possible.

The problem being solved here is to identify a set of suitable target asteroids and to find a trajectory to each, with launch and arrival dates and propulsive maneuvers defined, satisfying the performance and other mission constraints.

The mission has been divided into eight phases for planning purposes. The proposed design consists of a launch booster, which enters a low earth orbit (LEO) (a 200 km. altitude circular parking orbit is the baseline option), topped by a space vehicle consisting of a kick stage and spacecraft (Phase 1). The kick stage, with possibly some additional delta-v from the s/c, injects the latter into a hyperbolic escape trajectory leading to the earth's sphere of influence (SOI), in a burn called "delta-v 1" (Phase 2). See Fig. 1. Upon crossing the sphere of influence, the s/c travels on a heliocentric transfer orbit which

[+]Mission Analysis and Design, Commercial Satellite Operations, Lockhead Martin-Missiles and Space, Sunnyvale, CA 94089 Phone: (408) 742-9364 Fax: (408) 756-1223. Recent Ph.D. graduate of Dept. of AMES, UCSD.

[*]Professor Emeritus, Dept. of Applied Mechanics and Engineering Science (AMES), and NEAP team mentor at California Space Institute (CalSpace) headquartered at Univ. of Calif. at San Diego (UCSD), La Jolla, CA 92093. Phone: (619) 534-3181. FAX (619) 534-4543.

[++]Student members of NEAP design team at CalSpace, UCSD. In order, student manager, mission design, and propulsion system requirements. Phone: (619) 534-6463.

intersects the path of the asteroid at the nominal arrival date (Phase 3). A second s/c burn, "delta-v 2", achieves rendezvous, defined as matching the position and velocity of the asteroid. In actuality, delta-v 2 will be performed in increments over a one-month approach phase during which the closing speed relative to the asteroid is gradually reduced, and the angular velocity of the line-of-sight due to guidance and ephemeris errors is reduced to zero (Phase 4). When rendezvous has been accomplished, the s/c goes into the characterization phase (Phase 5), observing the asteroid with cameras and other science instruments, and dropping canisters with additional instruments onto the asteroid surface (Phase 6). In Phase 7, data is gathered from the surface canisters and other instruments, and relayed to earth. The eighth and final phase of the mission, in which the s/c lands on the asteroid, is carried out after the major objectives the mission have been achieved. Phases 5-8 will take a total of approximately 30 days.

The combined kick stage and s/c in the current design has a mass of 2000 kg and a delta-v capability of 7 km/sec, dictating the primary performance constraint of the mission, that the sum of delta-v 1 and delta-v 2 be less than this. Near-term arrival and scientific study of the asteroid is important to SpaceDev as a private business. Therefore, additional constraints are imposed, that launch occurs between July 1, 1999 and July 1, 2002 and that the mission time-of-flight is limited to 550 days maximum.

ASTEROID SELECTION PROCESS

It is intended that NEAP be designed to be able to visit any asteroid that meets the above constraints. This will maximize the chance of success since if schedule or launch difficulties cause us to miss our primary launch opportunity, another suitable one should be available within a few weeks or months. We must therefore identify all asteroid launch opportunities that meet our constraints.

The asteroid selection process can be divided into two phases. Phase I was an analysis and screening by the NEAP student team of the comprehensive Harvard-Smithsonian Center for Astrophysics collection of Near-Earth Objects, which numbered 416 at the time the study was carried out a few months ago. Asteroids were screened based on the total delta-v requirement, by launch date and by time-of-flight of the mission as indicated by the constraints above.

The process utilized a program prepared by one of us (C.C.), called NEAP 2. For one asteroid, NEAP 2 cycles through a series of launch dates covering the 3-year period of interest. For each launch date, it does an optimization minimizing the total delta-v as a function of asteroid arrival date. The optimization done in the NEAP 2 program utilized subroutines from "Numerical Recipes in Fortran" [1]. See Appendix. The program then outputs the data for the optimal trajectory for each launch date, including time-of-flight, delta-v 1, and total delta-v. A plot of this data for a sample asteroid appears in Fig. 2. Examination of this plot yields the launch date(s), if any, for which the total delta-v requirement falls within the design capability.

All asteroids from the 416 that met the total delta-v, launch date, and time-of-flight requirement were then considered in Phase II of the screening. These additional criteria were considered: date of arrival, solar panel area required (depending on the maximum range of s/c to sun over the mission), launch window size, and asteroid diameter (related to brightness and probability of detection by the camera sensor). The chief tool for orbit analysis in Phase II was another program (also by C.C.) called NEAP 3.

NEAP 3 constructs a trajectory for a single earth departure time and asteroid arrival time. It segments the trajectory into a user-specified number of intervals, equal in time, and writes information at each time step to an output file. This information includes the time since earth departure, the cartesian components of heliocentric position of the spacecraft, earth and asteroid, the distance of the spacecraft from the sun, earth, and asteroid, and the sun-spacecraft-earth angle. This output file is used to generate trajectory plots, and to determine such things as power and communications limitations based on distance from the sun and earth during the flight. It also provides the v-infinity vector at the earth's sphere of influence. The current reference trajectory for 1993 BX3 is shown in Fig. 3, projected onto the ecliptic plane.

All of the criteria defined earlier were used in Phase II of the selection process. These criteria varied widely among the Phase I asteroid candidates. A weighting method was developed to rank the candidate targets. A logarithmic function was assigned to each criterion. A sample weighting curve is shown in Fig. 4. Data from the NEAP 3 trajectory for a given candidate is used to enter the function, and the points for that criterion are computed. Points for each criterion are added to get the total point score. A high score signifies a good candidate. The score was computed for 22 of the top candidates. Our list, as of this date, appears in Table 1, with the asteroids listed in order of high priority to low. Because the Japanese work on the forthcoming MUSES-C mission is expected to produce an extensive analysis of Nereus (1982 DB), we have not included this asteroid in our planning.

Future changes to the weighting functions, and/or possible inclusion of additional factors, could change our preferences before the launch date. The uncertainty in the asteroid ephemeris data might be an important selection criterion. Any new criterion or modification to the weighing functions can easily be added to the program which computes the points and determines the ranking.

In this analysis a "point-conic" or zero sphere-of-influence model was used within the heliocentric frame-of-reference at the earth's position as well as at the asteroid. Accordingly, the spacecraft's position at the time of the escape maneuver is, in the heliocentric frame, simply the earth's position at that time. In the earth-centered frame, though, the escape maneuver is modeled as starting in a circular LEO parking orbit, with the two-body escape hyperbola and delta-v calculated for leaving this orbit with the speed and direction needed for the heliocentric requirements.

This difference in treatment between the two frames-of-reference can cause some confusion in interpreting the results, but the simplification of the heliocentric modeling is an aid to the analyst for exploring many asteroid and launch time possibilities within the fast pace of the NEAP program. The modeling error introduced by this simplification is small because of the short time spent in earth's vicinity relative to the total trajectory, and the accuracy is sufficient for this pre-design phase. Detailed and more accurate multibody simulation will necessarily have to be carried out before any flight is scheduled.

The velocity of the s/c with respect to the earth as it leaves the earth's sphere of influence is called "$\bar{v}_\infty$"; the vector sum of $\bar{v}_\infty$, and the velocity of the earth with respect to the sun, establish the initial velocity of the s/c in the heliocentric transfer orbit.

The magnitude of Δv_1 will vary depending on the asteroid selected and the launch date. Δv_1 ranges from about 3 km/sec to 6 km/sec. Some specific cases for Δv_1 are given in Table 2. The total Δv, which is the sum of Δv_1 and Δv_2, varies from 5 to 7 km/sec, depending on the asteroid selected.

LAUNCH AND ESCAPE TRAJECTORY PLANNING

The launch azimuth, the time of launch, the inclination of the LEO, the point in space where delta-v 1 must occur, and the v-infinity vector are all related in an interesting problem in solid geometry.

$\Delta\bar{v}_1$ is assumed to take place at the perigee of the hyperbolic escape trajectory. For propulsive efficiency, it is assumed that the initial parking orbit, the hyperbolic orbit, and $\Delta\bar{v}_1$, all lie in the same plane. Furthermore, it is assumed that $\Delta\bar{v}_1$ is tangential to both the initial parking orbit and the hyperbolic orbit. (Exception could be made to these principles provided sufficient propulsive capability exists in the launch vehicle.)

The discussion here is based on the principles enunciated in Bate, Mueller, and White [2]. However, a word of caution. Figures 8.3-4 and 8.3-5 in B,M,W, and shown here as Figs. 5 and 6, have been modified by replacing their "earth's orbital velocity vector" by our v-infinity vector. The v-infinity vector can have any direction in space, particularly if the asteroid orbital plane is inclined significantly relative to the ecliptic plane.

Consider the earth. From the center of the earth, draw a line in the direction $\bar{v}_\infty$. The line of action of $\bar{v}_\infty$ can be taken to be an axis of rotation. Any plane containing this line is a suitable plane for the initial parking orbit. Whatever plane finally selected to be the plane of the parking orbit then becomes the plane of the hyperbolic escape trajectory as well (adhering to the principles of efficiency described earlier).

In this plane, one backs off an angle η from the direction of $\bar{v}_\infty$. It is shown in [2] that η depends only on the eccentricity of the escape hyperbola, which in turn depends only on the magnitude of v_∞. Specifically,

$$\eta = \cos^{-1}\left[-\frac{1}{1+\frac{v_\infty^2 r_0}{\mu}}\right] \tag{1}$$

where r_0 is the radius of the perigee of the hyperbola, and μ is GM for the earth. The angle η is shown in Figs. 5 and 6. The significance of η is that it determines where the perigee point $\bar{r}_0$ of the hyperbola must be located. Subtracting η from π, we get another angle (β).

$$\beta = \pi - \eta \tag{2}$$

β is the half-angle of the cone shown sticking out of the earth in the opposite direction to $\bar{v}_\infty$ in Fig. 6. The first burn $\Delta\bar{v}_1$ occurs when the orbiting vehicle crosses the cone heading outward. Perigee of the parking orbit and perigee of the hyperbolic escape must be at the same point, and this point must lie on the surface of the cone.

It turns out that a plot of the angle β vs. v_∞ is very nearly a straight line (despite the non-linearity of equation (1)). Very nearly, for $\beta < 30^\circ$,

(3) $$\beta \cong 10\, v_\infty$$

where β is in degrees, and v_∞ is in km/sec. Equation (3) should not be used for precise work. It is only given so that one can perform back-of-the envelope calculations to get an idea of what an orbit will look like in a particular case.

Table 2 gives values of v_∞, β, Δv_1, and $\Delta\bar{v}_1$, for several launch date/asteroid combinations. In preparing this table, it is assumed that the launch into the parking orbit, and the time spent in the parking orbit, is zero (particularly, no more than a couple days). It is also assumed that r_0 =200 km altitude over the earth.

The inclination of the parking orbit is considered next. The desirable inclination varies from one asteroid launch opportunity to another. It is derived individually for each launch opportunity, and found by using the data in Table 2.

A rundown of Table 2 follows. Column 3 gives the magnitude of v-infinity (km/sec) of the s/c relative to the earth at the crossing of the SOI. The next three columns give the X,Y,Z components of the v-infinity vector in a coordinate system in which the X-Y plane is the ecliptic plane, with X directed toward the vernal equinox, and Y 90° east. The next two columns give the spherical coordinate angles of the v-infinity vector, that is, the celestial latitude and longitude (in degrees) measured north of the ecliptic plane and eastward from the vernal equinox. The next three columns give the v-infinity vector components in an inertially non-rotating, earth-centered, equatorial coordinate frame. This frame is sometimes referred to as the Earth-Centered Inertial (ECI) frame. In this frame, X and Y lie in the equatorial plane. The X axis is along the vernal equinox, and the Y axis is 90° east therefrom. Z is toward the north pole. (The data given in columns 9-13 is tentative - -we are still working to determine the correct conversion between this frame and the ecliptic, vernal equinox frame, based on the associated epochs.) Columns 12 and 13 give the declination and right ascension of the v-infinity vector in the ECI frame. Column 17 gives C_3 as the s/c leaves the earth's SOI. C_3 is twice the s/c energy (v-infinity squared for hyperbolic orbits).

As described earlier, the parking orbit plane must pass through the "anti-v-infinity" point. The anti-v-infinity point is the point of intersection of the v-infinity vector, projected backwards through the center of the earth, with an imaginary, inertially non-rotating, sphere surrounding the earth at an altitude of 200 km. This point is shown in Fig. 7 for a case in which the v-infinity vector points downward and to the rear. The right ascension of the anti-infinity point is obtained by adding or subtracting π from the right ascension of $\bar{v}_\infty$ (column 13). (Add π if the right ascension in column 13 lies between 0 and π. Subtract

π if the right ascension lies between π and 2π.) The declination of this point is found by reversing the sign of the declination of $\bar{v}_\infty$ (column 12).

Any orbit that passes through the anti-v-infinity point is a suitable parking orbit. Three such orbits (a,b, and c) are shown in Fig. 8 in terms of their great-circle trace on the imaginary sphere. All three orbits are proceeding eastward. Assume a direct ascent into a 200-km circular parking orbit from a given launch site, taken in this example to be located on the equator. Orbit (a) is obtained by launching earlier than the reference orbit. Orbit (b) is the reference orbit. Orbit (c) is obtained by launching later than the reference orbit. The inclination i of orbit (b) equals the absolute value of the declination δ of the anti-v-infinity point. Note the right spherical triangle GHJ in Fig. 8. The angle HJG, defined as the inclination i of orbit (b), is equal to the arc length HG=δ, the declination of the anti-v-infinity point H. The inclination of orbits (a) and (c) exceed the inclination of orbit (b). Thus, the minimum inclination of the parking orbit for the mission (assuming no plane change is made at Δv_1) is seen to be equal to the absolute value of the declination of the anti-v-infinity point.

In order to cause the parking orbit to achieve the right ascension of the anti-v-infinity point, a direct ascent launch must occur at precisely the right time of day. Since the earth rotates inside the imaginary sphere once every 24 hours, any given launch site will pass through the plane of the reference orbit (b), with an opportunity for launch in a northeasterly direction, once per day. There is also one opportunity each day to launch in a southeasterly direction. In other words, control of the right ascension is obtained by the time of launch, 0 to 24 hours. It can be seen that the tolerance on the launch time, i.e. the launch window, on any given day, is not very large, owing to the rotation of the earth through 1° every 4 minutes. One can open up the daily launch window by varying the launch azimuth, and hence the inclination of the parking orbit, with elapsed time on the launch pad. The nominal trajectory (b) is obtained by launching at that azimuth which establishes the inclination i equal to the declination of the anti-v-infinity point. The trajectory (a) is obtained by launching earlier than the nominal launch time into an orbit of larger inclination. The trajectory (c) is obtained by launching later than the nominal launch time, choosing a launch azimuth that also produces an inclination greater than i. The length of the launch window on a given day depends on the capability of the launch vehicle and its guidance system to achieve varying launch azimuths and parking orbit inclinations with the passage of time on the launch pad.

The Δv_1 burn occurs in the parking orbit after the space vehicle has passed the anti-v-infinity point, when it crosses the small circle of arc length β on the imaginary sphere. (That is, the radius of the circle has an arc length β on the surface of the sphere.) This circle is shown in Fig. 8. Thus, a' is where the burn will occur on trajectory (a), b' for (b), and c' for (c). In any one case, the velocity vector entering the burn, the Δv vector acquired during the burn, and the velocity vector leaving the burn are collinear, for propulsive efficiency, and furthermore, this burn should be locally horizontal, so that the burn point ("injection") becomes the perigee of the escape hyperbola. The launch vehicle must place the space vehicle into the correct orientation for the Δv_1 burn before separation.

It turns out that high inclinations for LEO are better than low, everything else being equal. Polar parking orbits can be used to reach any asteroid on our list, while equatorial

parking orbits are more limiting. The somewhat surprising conclusion came out of the analysis of the NEAP launch trajectory.

Future work may consist of searches for additional launch opportunities using three-burn trajectories and analysis of the effect of asteroid orbital element uncertainty on our selection and targeting process. It is unfortunate that some of the best asteroid candidates have been observed minimally and thus have large uncertainties in their elements. For missions after the first, we may consider low-thrust electric propulsion, and possibly the use of single or double-lunar swingbys, such as the approach in [3].

AJL
REFERENCES

[1] W. Press, S. Teukolsky , W. Vetterling and B. Flannery, "Numerical Recipes in Fortran," New York Second Edition, Cambridge University Press, 1992.

[2] R.R. Bate, D. D. Mueller and J.E. White, "Fundamentals of Astrodynamics," Dover, New York 1971.

[3] C.R. Cassell, "Optimization of Solar-Perturbed Double-Lunar-Swingby Escape Trajectories," Doctoral Thesis, Department of Applied Mechanics and Engineering Science, University of California, San Diego, June, 1997.

APPENDIX

Details of the NEAP 2 Optimization Process

The optimization done in the NEAP 2 program utilizes subroutines from "Numerical Recipes in Fortran" [1] for minimization of a function of a single parameter. The function constructed here, called "delv", returns the total delta-v, which is the sum of the LEO escape delta-v (dv1) and the asteroid rendezvous delta-v (dv2). The function's only argument is the Julian time of asteroid arrival. Other information that is needed to solve the trajectory satisfying the function call, or that is desired to be output through the main program, is passed through a Fortran Common Block. At the beginning of NEAP 2, the operator is prompted for the desired asteroid target, the range and increment of earth departure times to be considered, and for two times-of-flight to the asteroid. Then, for each departure time of the run, the Numerical Recipes subroutine "mnbrak" is called. This subroutine finds an interval of asteroid arrival time within which a minimum in total delta- v exists. The two input times-of-flight (translated to Julian asteroid arrival time) are used by mnbrak to start the search for this bracketing interval. The Numerical Recipes function "brent" is then called which makes repeated calls to "delv" until it converges to an asteroid arrival time within this interval that minimizes total delta-v.

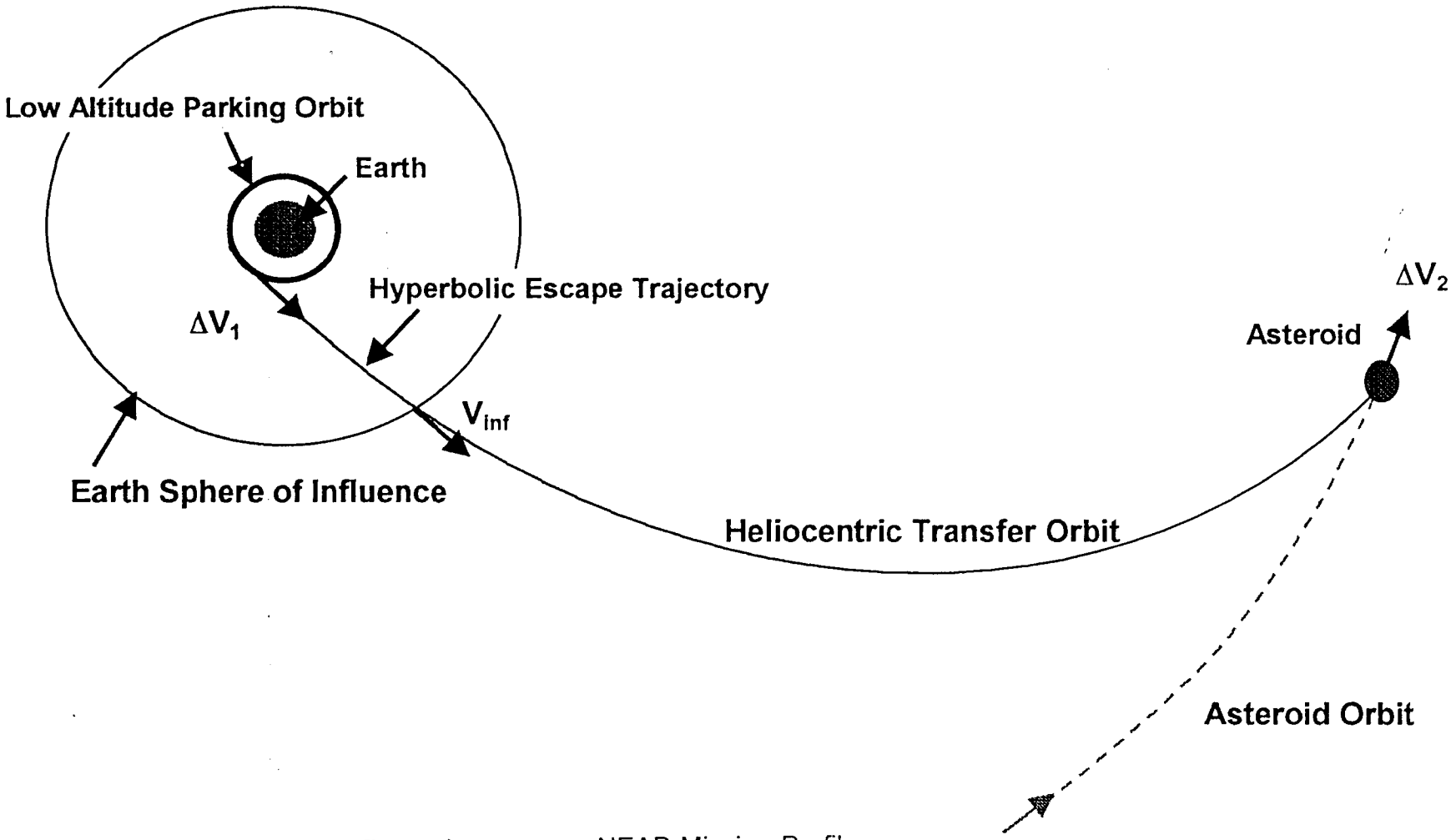

Figure 1 NEAP Mission Profile

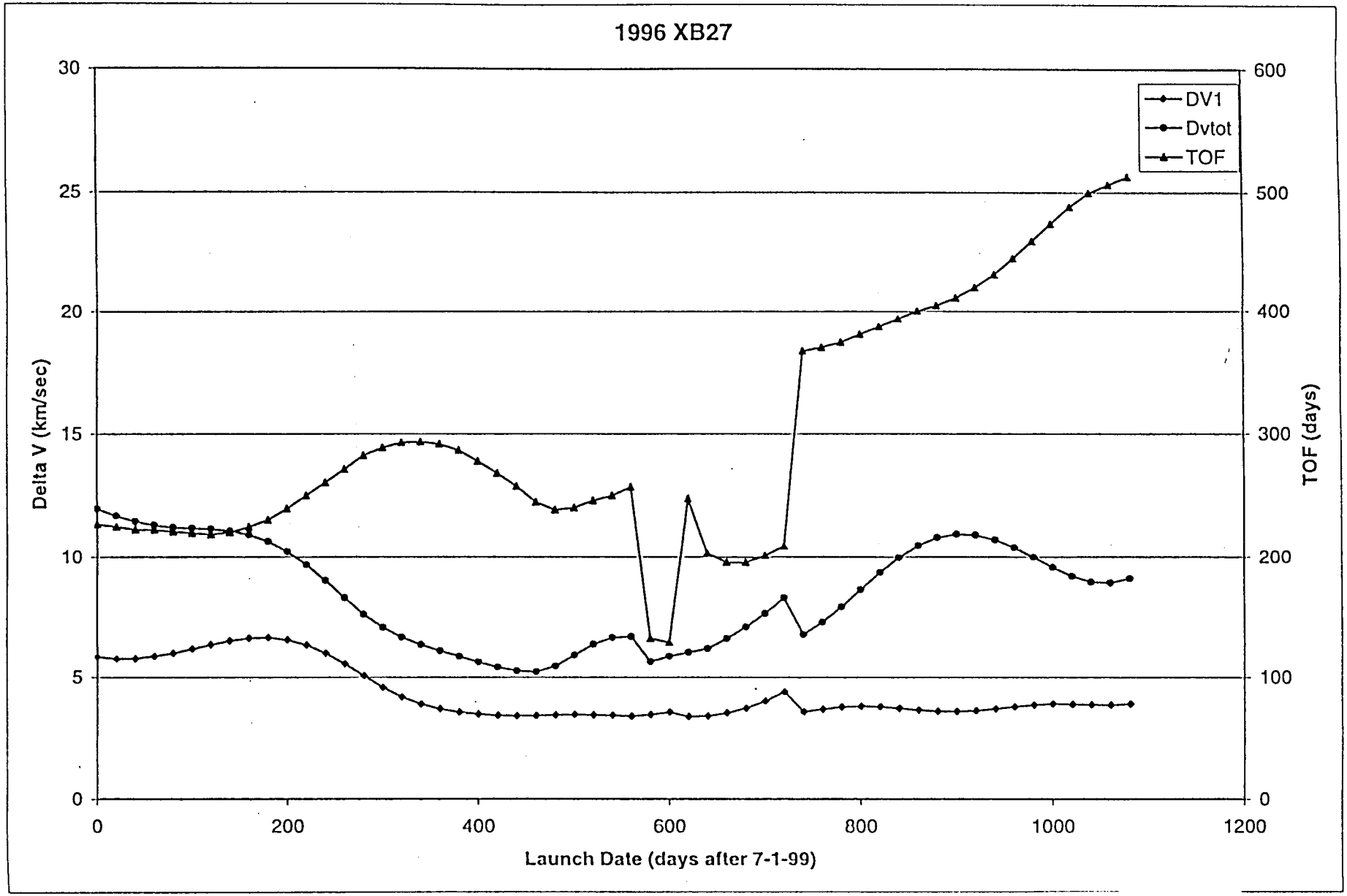

Figure 2 Time-of-flight, Delta-v 1, and Total Delta-v vs. Launch Date for 1996 XB27

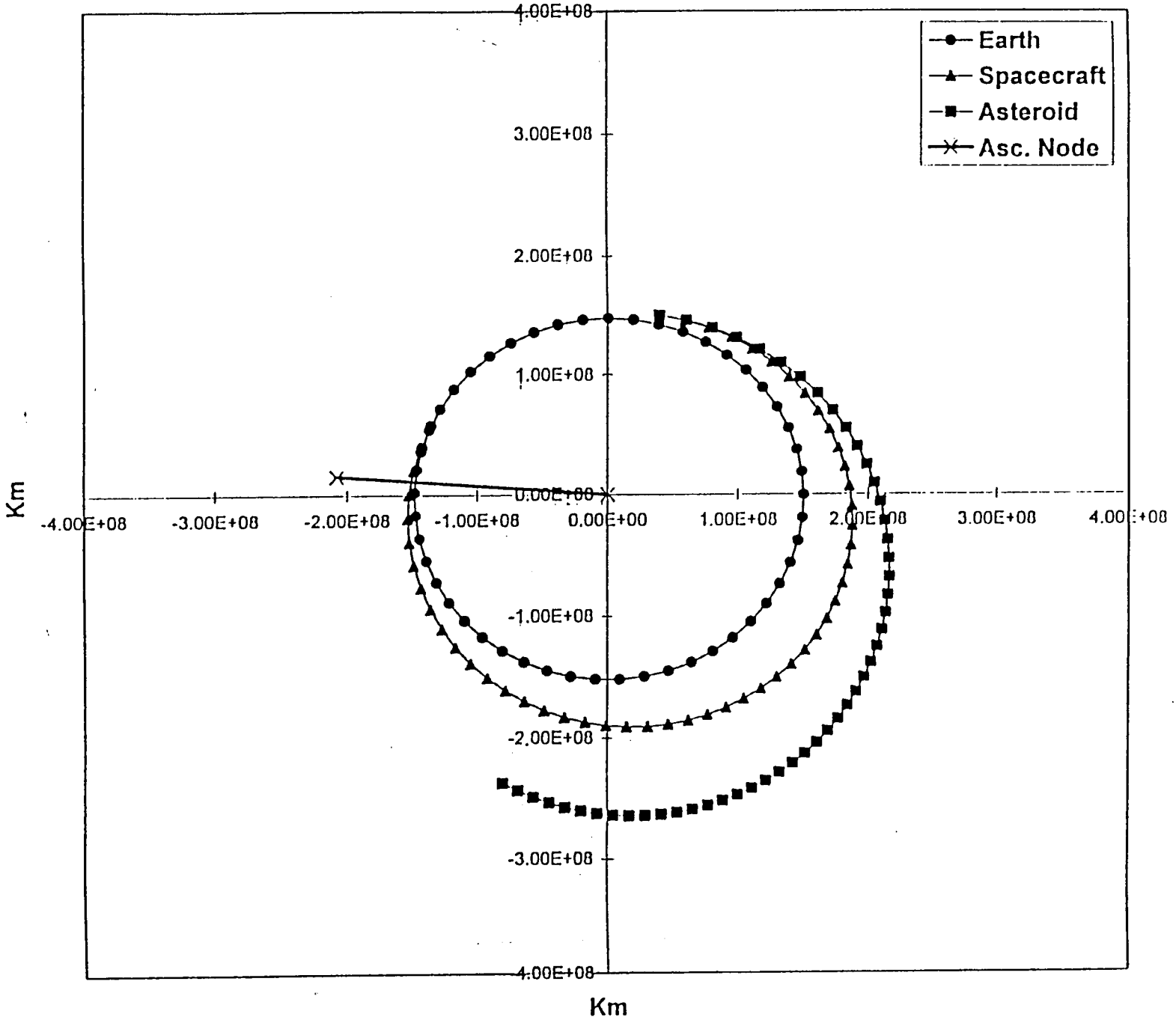

Figure 3 Trajectory to 1993 BX3. Marks represent evenly-spaced time points from first burn.

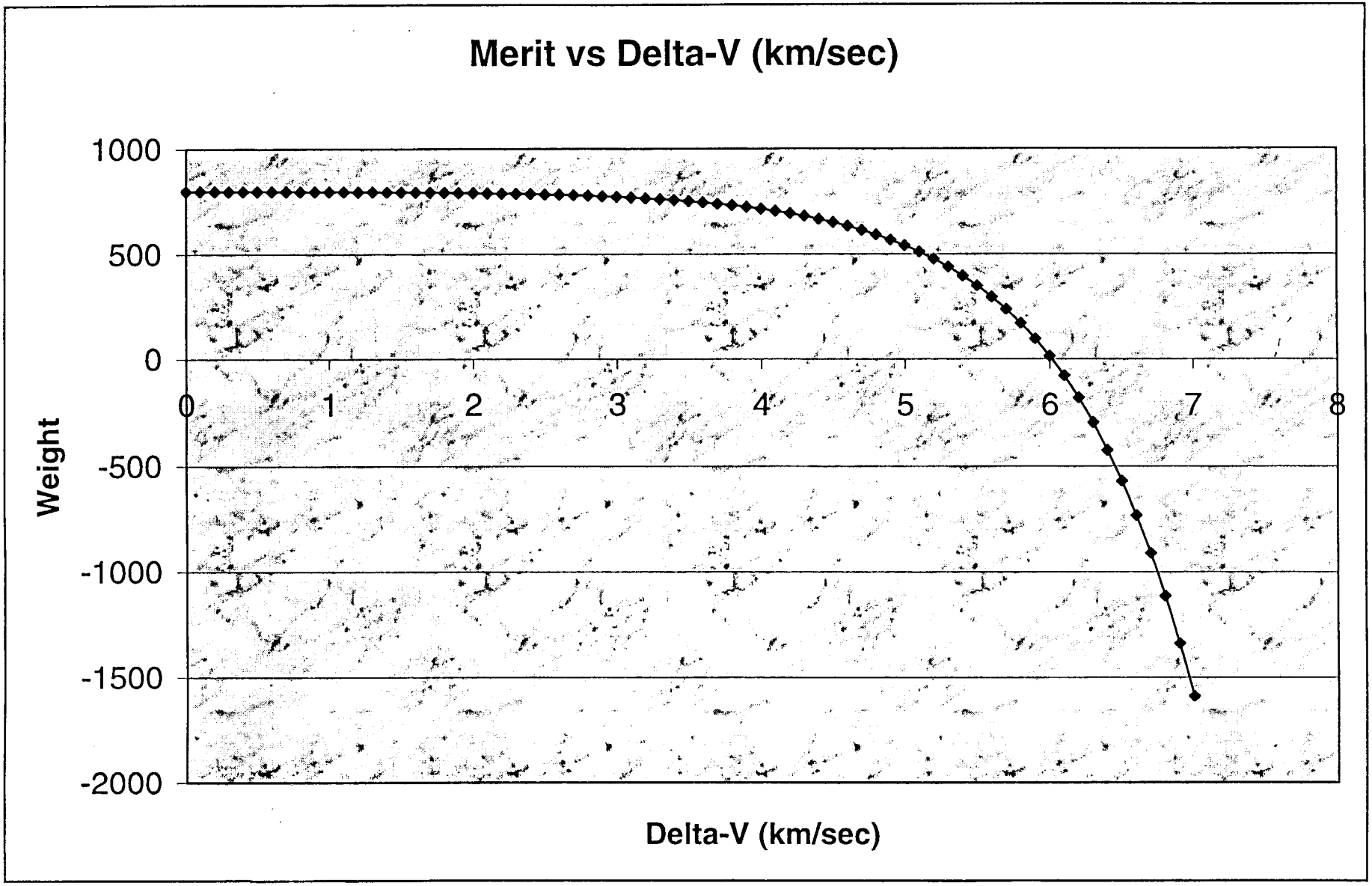

Figure 4 A Sample Weighting Curve

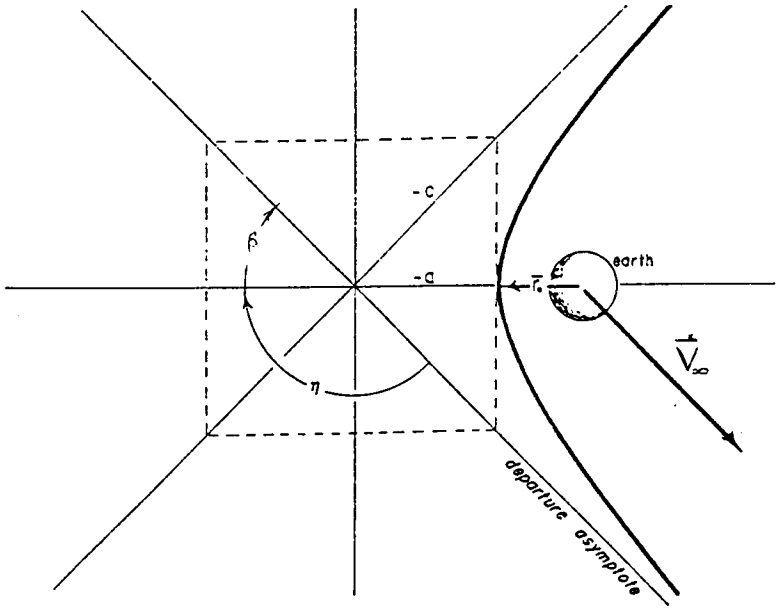

Figure 5 Geometry of the Departure Hyperbola

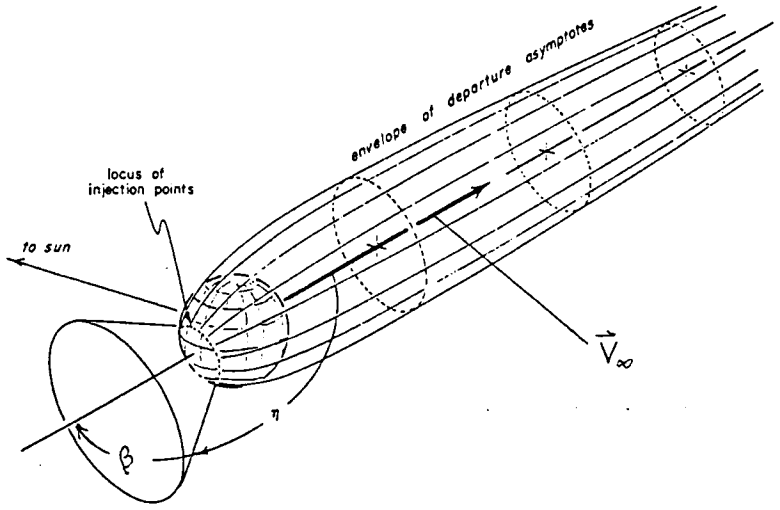

Figure 6 Locus of Possible Injection Points

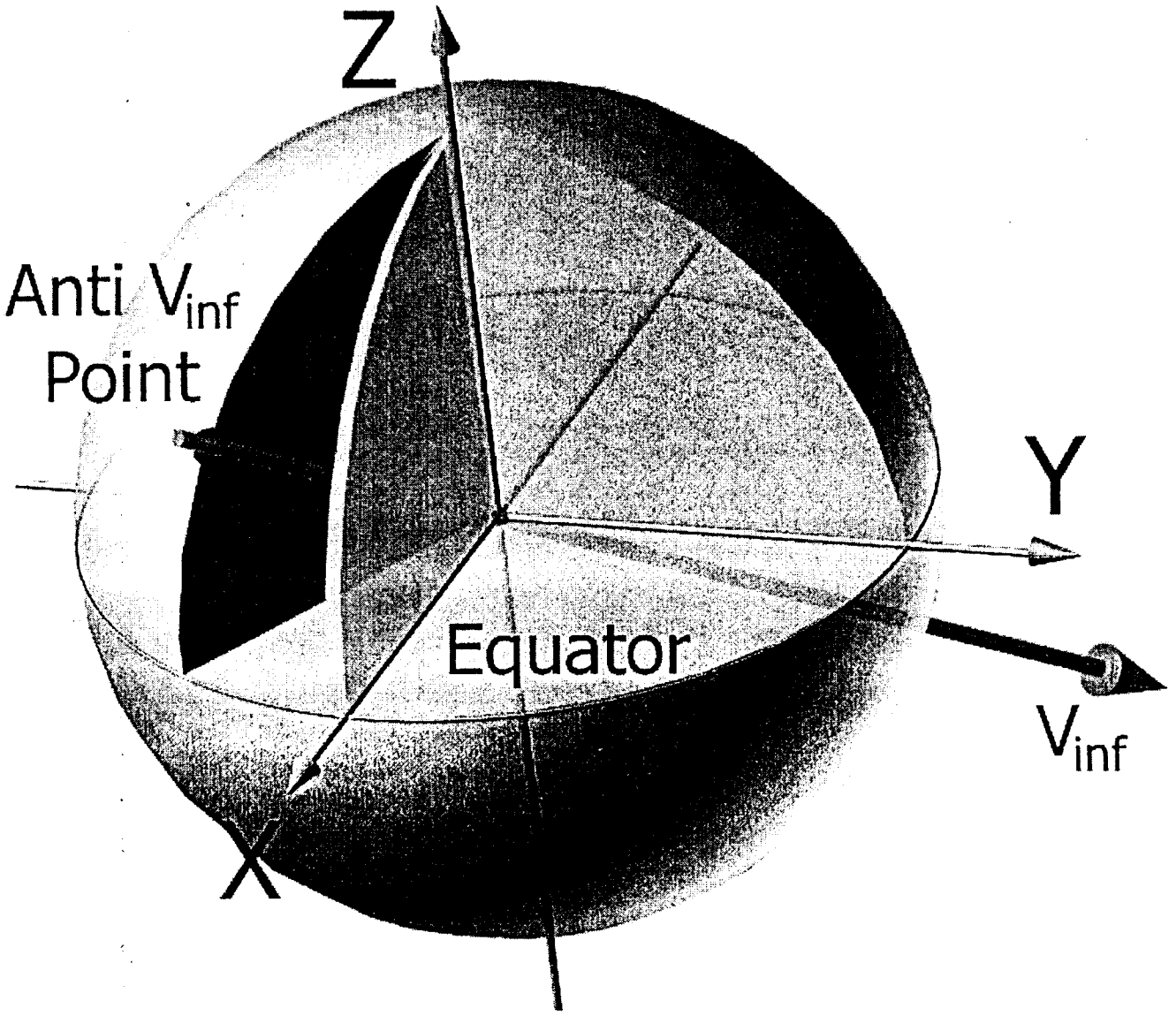

Figure 7 Anti-v-infinity Point

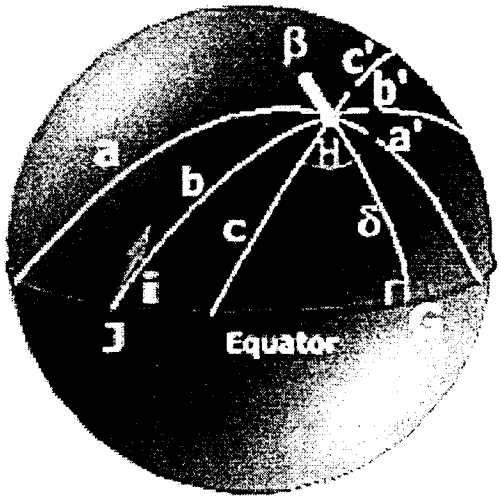

Figure 8 Three Suitable Parking Orbits and Their Launch Sites and Injection Points

Table 1
ASTEROID LAUNCH OPPORTUNITY PRIORITY

Trajectory Data																			Merit Values					
Asteroid	Launch Days after 7/1/99	TOF (days)	dv1 (km/s)	dv2 (km/s)	delvtot (km/s)	@ Asteroid (AU)	Furthest (AU)	Size (mag)	Est. Dia. (m)	Solar (m^2)	Launch Date Year	Month	Day	Arrival Date Year	Month	Day	A-day after 7/1/99	Days of Window	Delta-V	Arrival Date	Solar Panel Size	Launch Window	Asteroid Size	Total Merit
1993 BX3	240	374.29	3.574	2.184	5.757	1	1.3	20.5	340.0	1.8	2000	2	26	2001	3	6	614	111	199.89	319.54	244.86	97.74	-30.88	831.15
1996 XB27-2	460	244.87	3.400	1.825	5.225	1.1	1.1	22.0	175.0	1.6	2000	10	3	2001	6	4	705	374	467.78	246.33	245.72	128.11	-323.98	763.95
1996 XB27-3	580	132.03	3.450	2.193	5.643	1.12	1.12	22.0	175.0	1.36	2001	1	31	2001	6	12	712	374	271.74	238.27	246.56	128.11	-323.98	560.69
1996 GT	160	536.25	5.430	0.871	6.301	1.5	2	18.5	865.0	4.3	1999	12	8	2001	5	27	696	57	-297.60	255.51	200.15	81.08	259.64	498.78
1996 XB27-4	600	128.87	3.547	2.319	5.866	1.12	1.12	22.0	175.0	1.36	2001	2	20	2001	6	28	729	21	122.57	217.60	246.56	56.11	-323.98	318.85
1994 CN2-1	120	489.46	4.847	1.775	6.622	1	2	16.5	2000.0	4.3	1999	10	29	2001	3	1	609	33	-768.00	322.27	200.15	67.41	487.27	309.10
1996 FO3-3	240	387.54	3.803	2.812	6.615	1	1.3	18.5	865.0	1.8	2000	2	26	2001	3	19	628	45	-755.73	311.55	244.86	75.17	259.64	135.50
1994 CJ1	380	396.19	3.834	2.597	6.430	1	1.5	21.5	205.0	2.4	2000	7	15	2001	8	15	776	99	-467.32	144.25	241.14	94.88	-238.90	-225.95
1993 VA	180	538.75	4.331	2.491	6.822	1.5	2	17.3	1500.0	4.3	1999	12	28	2001	6	18	719	25	-1159.71	230.32	200.15	60.47	410.88	-257.90
1996 FG3-2	380	372.34	3.689	3.129	6.819	1.36	1.52	18.5	865.0	2.5	2000	7	15	2001	7	22	752	37	-1151.35	184.30	240.29	70.27	259.64	-396.83
1992 QN	620	336.53	4.877	1.738	6.615	1.6	1.7	17.0	1500.0	3.3	2001	3	12	2002	2	11	957	22	-756.48	-527.37	229.91	57.28	410.88	-585.78
1991 JR	700	193.79	4.813	1.464	6.277	1.5	1.5	22.5	135.0	2.9	2001	5	31	2001	12	10	894	34	-269.31	-192.44	236.04	68.16	-518.41	-675.96
1990 BA-1	260	425.66	3.754	3.156	6.909	1.2	1.7	18.0	415.0	3.1	2000	3	17	2001	5	16	686	32	-1357.42	266.04	233.25	66.64	37.35	-754.14
1977 VA-2	500	431.18	4.999	0.801	5.799	2.5	2.5	19.0	680.0	7.9	2000	11	12	2002	1	17	931	30	171.43	-373.78	-1065.30	65.03	190.33	-1012.29
1996 BG1-1	420	172.93	3.599	3.151	6.750	1.15	1.15	23.5	85.0	1.43	2000	8	24	2001	2	12	593	60	-1007.25	330.92	246.33	82.36	-850.00	-1197.64
1982 HR-1	680	276.21	4.033	2.808	6.841	0.83	1.12	19.0	680.0	1.36	2001	5	11	2002	2	11	956	31	-1200.32	-525.29	246.56	65.85	190.33	-1222.87
1996 XB27-1	300	288.76	4.579	2.478	7.057	1.18	1.19	22.0	175.0	1.53	2000	4	26	2001	2	8	589	374	-1743.02	332.95	245.98	128.11	-323.98	-1359.97
1977 VA-1	480	315.52	5.219	1.424	6.643	2.5	2.5	19.0	680.0	7.9	2000	10	23	2001	9	3	796	15	-805.97	106.38	-1065.30	47.70	190.33	-1526.86
1996 BG1-2	630	270.26	4.618	2.075	6.694	1.15	1.15	23.5	85	1.43	2001	3	22	2001	12	17	900	29	-898.44	-220.43	246.33	64.18	-850.00	-1658.35
1994 EU-1	620	359.90	3.787	2.977	6.764	0.99	1.13	25.5	35.0	1.38	2001	3	12	2002	3	6	980	32	-1036.97	-695.86	246.49	66.64	-850.00	-2269.69
1995 FG	300	353.82	4.681	2.312	6.993	2.2	2.2	23.0	105.0	6.1	2000	4	26	2001	4	14	654	8	-1567.46	293.28	-6.07	31.99	-1053.43	-2301.69
1980 AA	580	459.17	5.024	1.926	6.950	2.5	2.5	19.1	650.0	7.9	2001	1	31	2002	5	5	1039	45	-1457.52	-1273.43	-1065.30	75.17	177.02	-3544.05

Table 2
TRAJECTORY DATA FOR SEVERAL LAUNCH OPPORTUNITIES

	Asteroid	Launch Date	V_∞, magnitude	$V_{\infty X}$, ecliptic	$V_{\infty Y}$, ecliptic	$V_{\infty Z}$, ecliptic
1.)	1993 BX3	02/25/00	2.797	-2.083	-1.037	1.551
2.)	1996 XB27 #2	10/03/00	1.975	-1.248	0.360	-1.487
3.)	1996 XB27 #3	01/31/01	2.241	3.450	0.988	1.402
4.)	1996 GT	12/08/99	7.309	-2.655	6.467	2.132
5.)	1996 XB27 #4	02/20/01	2.685	-2.113	0.867	1.413
6.)	1996 FO3 #3	02/26/00	3.617	0.730	-1.830	-3.032
7.)	1994 CN2 #1	10/29/99	6.181	2.664	5.552	0.558
8.)	1994 CJ1	07/15/00	3.712	3.125	-1.836	-0.806

	V_∞, latitude	V_∞, longitude	$V_{\infty X}$, ECI	$V_{\infty Y}$, ECI	$V_{\infty Z}$, ECI	Declin. [deg]	right ascen. [deg]
1.)	33.695	206.473	-2.095	-1.545	1.021	21.41	216.41
2.)	-48.851	163.916	-1.244	0.936	-1.215	-37.97	143.05
3.)	38.732	145.598	-1.430	0.364	1.686	48.81	165.70
4.)	16.964	112.325	-2.576	5.114	4.541	38.42	116.74
5.)	31.742	157.695	-2.102	0.257	1.651	37.94	173.03
6.)	-56.982	291.738	0.707	-0.481	-3.514	-76.31	325.77
7.)	5.174	64.361	2.732	4.841	2.707	25.96	60.56
8.)	-12.540	329.562	3.102	-1.399	-1.485	-23.58	335.73

	ΔV_1 [km/sec]	ΔV_2 [km/sec]	ΔV_{total} [km/sec]	C_3 $[km/sec]^2$	η [deg]	β [deg]
1.)	3.569	2.190	5.759	7.717	152.502	27.497
2.)	3.400	1.825	5.225	3.899	159.975	20.024
3.)	3.450	2.193	5.643	5.02	157.442	22.557
4.)	5.430	0.871	6.301	53.42	122.104	57.895
5.)	3.547	2.319	5.866	7.21	153.337	26.662
6.)	3.803	2.812	6.615	13.08	145.332	34.667
7.)	4.847	1.775	6.622	38.21	127.826	52.173
8.)	3.834	2.597	6.43	13.78	144.559	35.44